EurJIC
European Journal of Inorganic Chemistry

A Journal of ChemPubSoc Europe

Accepted Article

Title: Catalytic cleavage of the amide bond in urea using a Co(III) amino-based complex

Authors: Bhawna Uprety, Charmaine Arderne, and Ivan Bernal

To be cited as: *Eur. J. Inorg. Chem.* 10.1002/ejic.201800975

Link to VoR: http://dx.doi.org/10.1002/ejic.201800975

WILEY-VCH

WILEY-VCH

FULL PAPER

Catalytic cleavage of the amide bond in urea using a Co(III) amino-based complex

Bhawna Uprety,[a] Charmaine Arderne,*[a] and Ivan Bernal[b]

Abstract: The urease mimetic activity of Co(III) amine complexes with respect to cleavage of urea was explored using SCXRD and spectroscopic techniques. The reaction of $[Co^{III}(tren)Cl_2]Cl$ (tren = tris(2-aminoethyl)amine) with urea results in the formation of an isocyanato complex ($[Co^{III}(tren)(NH_3)(NCO)]Cl_2$) and ammonia, following the cleavage of the amide bond. The reaction progress and the subsequent formation of cleavage products was confirmed by SCXRD analysis of the reactants as well as the products obtained during the reaction. The reaction was found to be pH and temperature dependent, and the reaction conditions were optimized to maximize conversion. The reaction kinetics was followed spectroscopically (^{1}H NMR and UV-Vis), following the decrease in urea concentration or the increase in pH succeeding ammonia formation. A detailed kinetic study revealed an overall second order rate law and k_{obs} was found to be 3.89×10^{-4} M^{-1} s^{-1}.

Introduction

Urease (urea amidohydrolase; E.C.3.5.1.5) is a nickel–dependent dinuclear metallohydrolases, present in various plants and microorganisms, that catalyses the hydrolysis of urea to ammonia and carbon dioxide (and small amides to the corresponding carboxylic acids)[1–4]. This enzymatic hydrolysis causes an abrupt increase of pH, having direct medical and agricultural consequences[3–6]. The enzyme plays vital roles in nitrogen metabolism of plants and microorganisms[7,8]. Urease is an interestingly skilled enzyme system, since its substrate urea, has a remarkable stability with a half-life of about 3.6 years; and it does not undergo spontaneous hydrolysis in aqueous solutions[9,10]. Instead its aqueous decomposition follows an elimination route, giving isocyanic acid or ammonium cyanate as one of the reaction products irrespective of the pH of the solution[7,11–13]. However, this non catalytic elimination proceeds sluggishly with a rate constant ranging from 8.3×10^{-10} – 1.2×10^{-11} s^{-1} at 25 °C[14,15].

[a] B, Uprety; C, Arderne
Department of Chemistry
University of Johannesburg
PO Box 524, Auckland Park 2006, Johannesburg, South Africa
E-mail: carderne@uj.ac.za

[b] I, Bernal
Molecular Sciences Institute, School of Chemistry
University of the Witwatersrand, 2050
Johannesburg, South Africa

Supporting information for this article is given via a link at the end of the document.

At the active site, Urease contains two nickel ions bridged by a carbamylated lysine and a hydroxide ion[16–18]. Although, the exact mechanism of its action is still under debate, there are two globally accepted hypotheses. The first is: urea binds to one of the Ni centres through its carbonyl moiety, while the hydroxide coordinated to the second Ni then initiates a nucleophilic attack on urea, thus beginning the hydrolysis reaction. The second is: urea coordinates in a bidentate fashion to one of the Ni(II) centres and an amino acid residue on the second Ni(II) centre, leaving the hydroxide bridge intact. The hydroxide bridge then attacks the urea carbonyl group in a nucleophilic manner, initiating the hydrolysis[9,19–22]. Subsequently, the coordinated hydroxide ligand is crucial to the active site of Urease. This observation might play a pivotal role in designing synthetic Urease mimics, as was evident in our study as well. There is sufficient evidence of several Urease mimics based on polydentate as well as linear ligands documented in literature. Most of them report the coordination of urea to the metal centres via the carbonyl oxygen while coordination via nitrogen is rather scarce[23–26]. Nevertheless, the majority of synthetic urease mimics follow an elimination mechanism giving iso/cyanates as the major products along with ammonia, and therefore designing of a true Urease mimic has been an intriguing challenge globally. However, in a few cases, the subsequent decomposition of iso/cyanates into carbon dioxide and ammonia under suitable reaction conditions has also been observed[25,27–29].

Recently, there has been an emerging interest in the catalytic activity of Cobalt (III) complexes[30–32]. The mechanistic studies suggest catalytic activation *via* different kinds of interactions with diverse organic substrates[33]. The applicability of Co(III) amine complexes towards mediating peptide/amide bond hydrolysis in carnosine and pyrazine–2–monoamide, salicylaldehyde, etc. have been reported recently by some of us[34–36]. This encouraged us to examine whether these Co(III) amine complexes could also hydrolyse urea; and if so, could we determine the underlying mechanistic and/or kinetic pathways. Therefore, this study focuses on the catalytic activity of a compound of the tris(2-aminoethyl)amine (tren) ligand complexed to a Co(III) metal centre on urea.

Results and Discussion

$[Co^{III}(tren)Cl_2]Cl$ (**1**) was prepared in excellent yields following a two–step synthetic method as reported in literature[37]. The intermediate nitro complex, $[Co^{III}(tren)(NO_2)_2]Cl$[38] (**1a**) as well as the final $[Co^{III}(tren)Cl_2]Cl$ (**1**) compound, were well characterized

by various spectroscopic techniques (FT–IR, NMR, UV–Vis, HRMS) as well as by Single-crystal XRD (SCXRD) analysis. They are both air stable solids soluble in water, and sparingly soluble in alcohols. Compound (**1**) was recrystallized from both water and concentrated HCl (32%), resulting in two different complexes, $([Co^{III}(tren)Cl_2]Cl)_2\cdot(Cl)(H_7O_3)$, (**$((1)_2\cdot(Cl)(H_7O_3))$**) and $[Co^{III}(tren)Cl_2]Cl\cdot H_2O$, (**$1\cdot H_2O$**) respectively. The first is complex (I): Dichloro(tris-2-amino(ethylamine))cobalt(III) chloride hydrate whose crystals were obtained from the reaction mixture mother liquor and recrystallized from 32% HCl. The second is complex (II): *Bis-(*dichloro(tris-2-amino(ethylamine))cobalt(III)dichloride) dihydrate hydroxonium chloride whose crystals were obtained from the reaction mixture mother liquor and recrystallized from water. Therefore, the solvent of crystallization plays an important role in stabilizing the resulting structure of the compound. This was corroborated by recording the HRMS (Figures S1 and S2) of the complex before and after crystallization. The HRMS spectrum of the crude compound before crystallization displays an intense peak at 275.0232 which corresponds to $[Co^{III}(tren)Cl_2]$ (calc. 275.0241). However, the HRMS spectrum for the complex (II) obtained after crystallization from water, has an intense molecular ion peak at 735.1824 which can be attributed to $([Co^{III}(tren)Cl_2]Cl)_2\cdot(Cl)(3H_2O)(Na)$ (calc. 735.5320) in solution. All reactions of $[Co^{III}(tren)Cl_2]Cl$ (**1**) were carried out using complex (II), $([Co^{III}(tren)Cl_2]Cl)_2\cdot(Cl)(H_7O_3)$, (**$((1)_2\cdot(Cl)(H_7O_3))$**), as we reasoned that since our reactions were aqueous, we should use catalysts purified from water. The crystal structures of both complex ($1\cdot H_2O$) and ($(1)_2\cdot(Cl)(H_7O_3)$) are presented and discussed in this work for completeness.

The application of Co(III) amine complexes similar to $[Co^{III}(tren)Cl_2]Cl$ (**1**) towards hydrolysis of several bio–relevant substrates such as phosphoesters, phosphodiesters, as well as some dipeptides etc. are well documented in literature[34–36,39–41]. The present work explores the ability of $[Co^{III}(tren)Cl_2]Cl$ (**1**) to catalyse the hydrolysis of amide bonds. For this purpose, we have employed the simplest amide molecule – urea (Scheme 1). The catalytic reactions were monitored by ^1H NMR as well as UV–Vis spectroscopy following the decrease in Urea concentration and the formation of ammonia respectively.

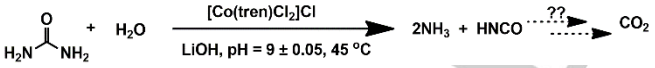

Scheme 1. Hydrolysis of urea at pH 9 ± 0.05 in the presence of LiOH and catalysed by $([Co^{III}(tren)Cl_2]Cl)_2\cdot(Cl)(H_7O_3)$ (**$((1)_2\cdot(Cl)(H_7O_3))$**) at 45 °C in water.

Catalytic hydrolysis of urea: UV–Vis studies

Urease like hydrolysis of urea yields ammonia and carbamate which decomposes to yield a second molecule of ammonia and bicarbonate. The catalytic reaction induces an overall increase in pH[3]; consequently, the reaction progress can be monitored passively, with the help of a pH dependent colour indicator assay. Similar Urease studies involving different pH dependent indicator assays such as phenol red and phenolphthalein are well documented in literature[4,8,42,43]. We have performed our reactions using phenolphthalein indicator assay to measure the catalytic activity of $([Co^{III}(tren)Cl_2]Cl)_2\cdot(Cl)(H_7O_3)$ (**$((1)_2\cdot(Cl)(H_7O_3))$**). Phenolphthalein is a good indicator of choice in this case, since it shows a visible colour change in alkaline pH range 8.2 – 12. The catalytic reactions were performed at pH 9 ± 0.05 in the presence of hydroxide ions. Interestingly, no reaction was observed in the absence of hydroxide, whereas the reaction was too slow to be quantified at lower pH ranges.

In a typical reaction, an aqueous solution of $([Co^{III}(tren)Cl_2]Cl)_2\cdot(Cl)(H_7O_3)$ (**$((1)_2\cdot(Cl)(H_7O_3))$**), (10 mL, 4.5×10^{-4} M) was set to pH 9 ± 0.05 using 1 % LiOH solution, and was then allowed to incubate at the same pH at room temperature for about 1 hr, to stabilize the pH of the solution. Over the 1 hr of incubation, the colour of the solution changed from purple to red indicating the complete replacement of coordinated chlorides to the aqua and/or hydroxide ligands. This conversion was also monitored by UV–Visible spectroscopy following the progressive addition of LiOH solution to a solution of $([Co^{III}(tren)Cl_2]Cl)_2\cdot(Cl)(H_7O_3)$ (**$((1)_2\cdot(Cl)(H_7O_3))$**) in water; and the results are presented in supplementary information (Figure S3). Next, an aqueous solution of urea (2 mL, 1×10^{-2} M) was mixed with a pH adjusted aqueous solution of the catalyst (2 mL, 4.5×10^{-4} M). The pH of the reaction mixture at this stage was still 9 ± 0.05. Phenolphthalein indicator (1 mL, 1 %) was added to this solution and the resulting reaction mixture was incubated at 45 °C. The reaction was then followed by monitoring the increase in absorbance at 552 nm, due to the alkaline quinone form of phenolphthalein which is only prevalent at basic pH, for a period of 1 hr to obtain initial rates for the relevant kinetic calculations. (Figure 1).

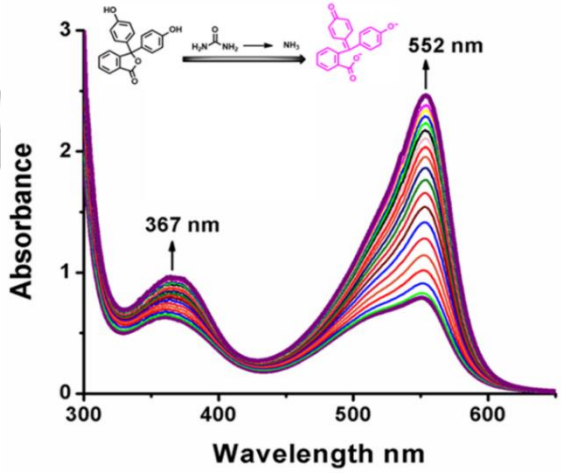

Figure 1. Increase in absorbance at 552 nm and the progress of reaction as monitored by UV–Visible spectroscopy with the aid of phenolphthalein indicator.

Co(III) chlorido systems are known to undergo rapid hydrolysis in aqueous systems, giving the corresponding $[Co^{III}(L)(OH)(H_2O)]^{2+}$ species in solution. The $[Co^{III}(L)(OH)(H_2O)]^{2+}$ species is believed to be the dominant species at alkaline pH and is actively involved in catalysing hydrolysis reactions[44]. This can be corroborated with the actual Urease enzyme activity; where the carbamate bridge between the two Ni centres is hydrolysed to a hydroxide bridge initiating the catalytic activity in Urease[16–18]. Therefore, formation of the hydroxido active intermediate can be considered crucial to catalytic activity. This can partly explain the inactivity of

the precursor $[Co^{III}(tren)(NO_2)_2]Cl$ (**1a**) complex towards urea hydrolysis, since the nitro groups are resistant to hydrolysis under alkaline aqueous conditions. The formation of this active intermediate hydroxide species in solution during our reaction, was followed by sequential additions of an aqueous solution of LiOH (1×10^{-3} M) to an aqueous solution of $([Co^{III}(tren)Cl_2]Cl)_2{\cdot}(Cl)(H_7O_3)$ (**$(1)_2{\cdot}(Cl)(H_7O_3)$**), (25 mL, 4.5×10^{-4} M) at room temperature. The reaction was monitored by UV–Visible spectroscopy and the results are included in the SI section.

The catalytic reaction conditions were optimized to maximize reaction conversion. For this, some reaction parameters such as reaction pH, temperature and catalyst amount were evaluated. As mentioned earlier, the reaction was too slow at pH below 9 to be quantified kinetically. The reaction did not proceed at all at acidic pH; therefore, the reaction pH was incubated to alkaline pH using the mild base LiOH. Similar results have been reported by some of us, in the investigation of conglomerate crystallization, where the cleavage of amide bonds in small peptide molecules mediated by $[Co(tren)Cl_2]Cl$ was observed[34–36]. Therefore, a reaction pH of 9 ± 0.05 was concluded essential for catalytic activity.

Next, the effect of catalyst concentration was evaluated. A set of different reactions, with the same conditions as described above, but with varying catalyst concentration were performed. The reaction progress was monitored by UV–Visible spectroscopy as described above. Three parallel reactions were set using 4.5×10^{-5} M, 4.5×10^{-4} M and 4.5×10^{-3} M catalyst concentrations (~ 1:1000, 1:100, 1:10 catalyst : substrate ratio respectively) set at pH 9 ± 0.05 with LiOH and 1×10^{-2} M urea solution at 45 °C in the presence of phenolphthalein indicator (1 ml, 1%). The resulting spectral changes are presented in Figure 2. As can be seen from Figure 2, increasing the catalyst concentration increased the rate of the reaction, a common observation in catalysed reactions. However, to perform kinetic studies, and have quantifiable results, the average ratio (~ 1:100) for catalyst and substrate concentration was chosen for kinetic experiments.

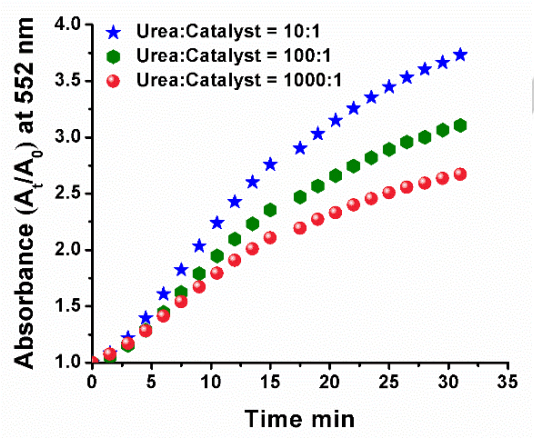

Figure 2. Change in absorbance at 552 nm during the course of reaction, with different catalyst to substrate ratios.

However, the reaction was also performed with larger quantities, in an attempt to isolate any possible intermediates and/or products. Therefore, to an aqueous solution of urea (17 mmol, 30 mL) was added 0.535 g (0.75 mmol) of $([Co^{III}(tren)Cl_2]Cl)_2{\cdot}(Cl)(H_7O_3)$ (**$(1)_2{\cdot}(Cl)(H_7O_3)$**). The pH of the resulting solution was set to 9 ± 0.05 with freshly prepared 10 % LiOH solution, and the solution was stirred at 45 °C for about 2 hr. The reaction was then allowed to cool and stand at room temperature, for a few days, after which diffraction quality orange rod–like crystals precipitated out. The isolated product, has a molecule of ammonia and an isocyanato group coordinated to the metal centre, along with the base ligand, tris(2–aminoethyl)amine $[Co^{III}(tren)(NH_3)(NCO)]Cl_2$ (**2**). The isocyanic acid and ammonia are proposed to be the catalytic products of urea cleavage reactions.

Next, the effect of temperature on the reaction rates was evaluated. For this, six reactions, with the conditions as described above, but with temperatures between 20 – 45 °C were performed. Thus, a solution of urea (2 mL, 1×10^{-2} M) was treated with a solution of $([Co^{III}(tren)Cl_2]Cl)_2{\cdot}(Cl)(H_7O_3)$ (**$(1)_2{\cdot}(Cl)(H_7O_3)$**) (2 mL, 4.5×10^{-4} M) set at pH 9 ± 0.05 with LiOH at six temperatures, 20 °C, 25 °C, 30 °C, 35 °C, 40 °C and 45 °C in the presence of phenolphthalein indicator (1 ml, 1%). The reactions were monitored by UV–Visible spectroscopy on a kinetic run mode and the initial rates were obtained as triplicates assuming pseudo first order kinetics. As can be seen from Figure 3, the rate of the reaction increased with increasing temperature and thus 45 °C was chosen as the ideal temperature for catalytic activity.

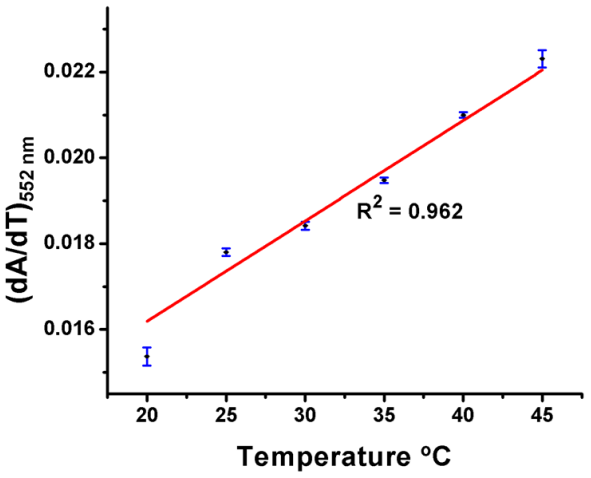

Figure 3. Effect of temperature on the increment in absorbance at 552 nm with time for the hydrolysis of urea (1×10^{-2} M) catalysed by $([Co^{III}(tren)Cl_2]Cl)_2{\cdot}(Cl)(H_7O_3)$ (**$(1)_2{\cdot}(Cl)(H_7O_3)$**) (4.5×10^{-4} M) at pH 9 ± 0.05, in the presence of LiOH, at temperature ranging from 20 – 45 °C.

Furthermore, the initial rates obtained at different temperatures were then fitted to the Arrhenius equation, according to equation 1 (Figure 4). The activation energy, E_a, for the generation of ammonia during the initial steps of urea hydrolysis was found to be 10.2 kJ mol^{-1}. The literature activation energy values for the actual Urease enzyme ranges between 18 – 30 kJ mol^{-1}[42]. The optimised temperature and

pH for the catalytic reaction were found to be considerably higher than the enzymatic hydrolysis. The intermediate isolated during the catalytic reaction, $[Co^{III}(tren)(NH_3)(NCO)]Cl_2$ (**2**) contains isocyanato and ammonia ligands coordinated to the metal centre, both of which are proposed to result from an elimination mechanism rather than hydrolytic cleavage of urea (*vide infra*).

$k = A \exp(-Ea/RT)$ Equation (1)

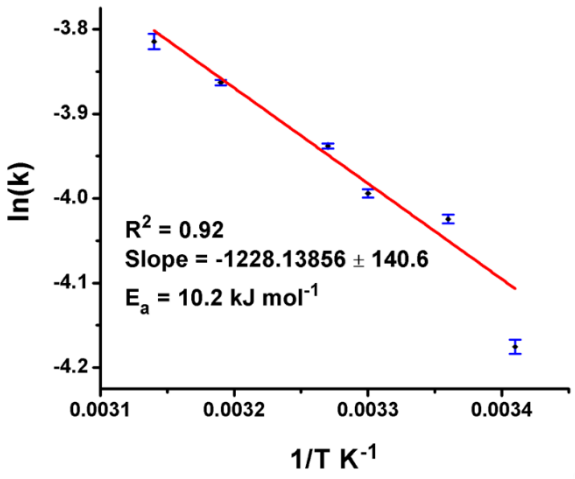

Figure 4. Arrhenius plot for $([Co^{III}(tren)Cl_2]Cl)_2{\cdot}(Cl)(H_7O_3)$ (**$(1)_2{\cdot}(Cl)(H_7O_3)$**) catalysed hydrolysis of urea at pH 9 ± 0.05. Reaction conditions: urea (2 ml, 1×10^{-2} M), $[Co(tren)Cl_2]Cl$ (2 mL, 4.5×10^{-4} M), phenolphthalein (1 ml, 1%), temperature ranging from 20 – 45 °C.

Catalytic hydrolysis of urea: NMR studies

The catalytic hydrolysis of urea was also followed by ^{1}H NMR spectroscopic reaction monitoring. The reaction progress was analysed by following the decrease in urea concentration over time. In a typical reaction, urea (0.240 g, 4.0 mmol) was added to a solution of $([Co^{III}(tren)Cl_2]Cl)_2{\cdot}(Cl)(H_7O_3)$ (**$(1)_2{\cdot}(Cl)(H_7O_3)$**) (0.124 g, 0.17 mmol, 10 mL D_2O) and adjusted to pH 9 ± 0.05 with LiOH. A small aliquot of the reaction mixture (0.5 µL) was withdrawn into an NMR tube and analysed by ^{1}H NMR spectroscopy at 45 °C in the presence of CH_3OD as the internal reference, every 15 minutes on a 12 hr time scale. Figure 5 presents the spectral changes during the initial two hours.

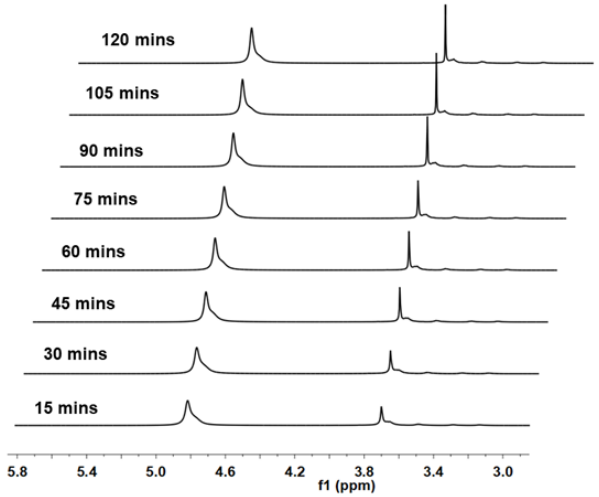

Figure 5. ^{1}H NMR monitoring of the hydrolysis of urea catalysed by $([Co^{III}(tren)Cl_2]Cl)_2{\cdot}(Cl)(H_7O_3)$ (**$(1)_2{\cdot}(Cl)(H_7O_3)$**) at pH 9 ± 0.05, in the presence of LiOH, at 45 °C. Reaction conditions: urea (4 mmol), $([Co^{III}(tren)Cl_2]Cl)_2{\cdot}(Cl)(H_7O_3)$ (**$(1)_2{\cdot}(Cl)(H_7O_3)$**) (0.17 mmol), pH 9 ± 0.05, temperature 45 °C, solvent D_2O + CH_3OD. (The signals for the catalyst are not seen prominently due to low concentration as compared to the catalyst as well as the internal standard)

As the reaction progressed, the intensity of the urea signal decreased over time. The formation of ammonia could not be ascertained from ^{1}H NMR studies, since the reactions were performed in D_2O, and therefore the ammonia protons could not be seen in the spectra. It is important to note that although the urea amine protons also merge with the signal for D_2O, the integration with respect to the internal standard at t = 0 time was six, allowing a possible kinetic monitoring of the reaction, following the decrease in urea concentration. The reaction was monitored for a period of 12 hr during which a total conversion of 60 % was estimated. However, since the signals for ammonia protons could not be properly identified, the exact conversion cannot be stated unequivocally.

All kinetic calculations were performed assuming pseudo first order kinetics, thus maintaining an ~ 25-fold excess of substrate concentration with respect to the catalyst concentration. All calculations were performed using initial reaction rates. The rate of the catalytic reaction can be obtained by considering the integrated rate law (equation 2). The plot of log of decrease in concentration of urea with time is shown in Figure 6. Since the concentration of the catalyst can be assumed to be remaining almost constant during the reaction, the reaction can be assumed to be following first order kinetics with respect to the substrate, i.e. urea. This is also apparent from the straight-line fit obtained in Figure 6. Consequently, the resulting pseudo first order rate constant was found to be 3.5×10^{-5} s^{-1}.

$\text{Rate} = k_{obs}[\text{Urea}]^a[\text{Catalyst}]^b$ Equation (2)

$\text{Rate} = k_1[\text{Urea}]^a$

(assuming pseudo first order kinetics) Equation (3)

where $k_1 = k_{obs}[\text{Catalyst}]^b$ Equation (4)

$\ln k_1 = \ln k_{obs} + b\ln[\text{Catalyst}]$ Equation (5)

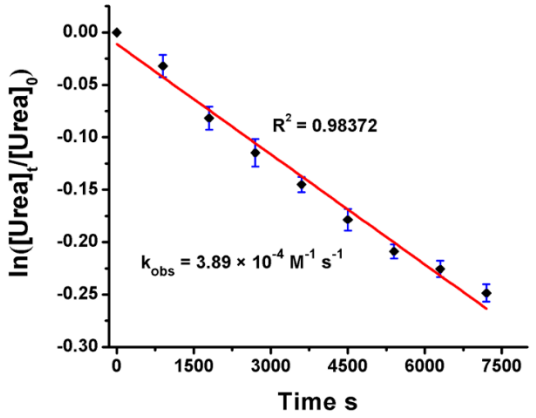

Figure 6. Variation of [Urea] with time for the catalytic hydrolysis reaction of urea catalysed by $([Co^{III}(tren)Cl_2]Cl)_2{\cdot}(Cl)(H_7O_3)$ (**$(1)_2{\cdot}(Cl)(H_7O_3)$**) at pH 9 ± 0.05, in the presence of LiOH, at 45 °C. Reaction conditions: $[Urea]_0$ = 4 mmol, [catalyst] = (0.17 mmol), solvent D_2O + CH_3OD.

Using equations 2 – 5, the order of the reaction with respect to the catalyst can also be determined. Thus, the initial rates for the hydrolysis of urea by $([Co^{III}(tren)Cl_2]Cl)_2{\cdot}(Cl)(H_7O_3)$ (**$(1)_2{\cdot}(Cl)(H_7O_3)$**) at pH 9 ± 0.05, in the presence of LiOH, at 45 °C were determined for different initial concentrations of the catalyst (and consequently LiOH). The reactions were performed similarly as explained above and the resulting plot from equation 5 is shown in Figure 7. Thus, the order of the reaction with respect to the catalyst was found to be 0.81, and k_{obs} for the catalytic hydrolysis of urea was found to be 3.89 × 10^{-4} M^{-1} s^{-1}.

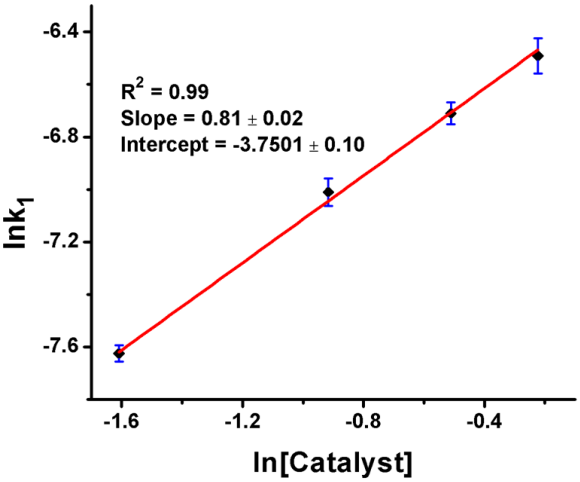

Figure 7. Plot of ln k_1 versus ln[catalyst] for the hydrolysis of urea catalysed by $([Co^{III}(tren)Cl_2]Cl)_2{\cdot}(Cl)(H_7O_3)$ (**$(1)_2{\cdot}(Cl)(H_7O_3)$**) at pH 9 ± 0.05, in the presence of LiOH, at 45 °C.

The overall integrated rate law for the hydrolysis of urea in the presence of excess alkali can be represented as:

$$\text{Rate} = k_{obs}[\text{Urea}][\text{catalyst}] \quad \text{at 45 °C and pH} = 9 \pm 0.05.$$

$$k_{obs} = 3.89 \times 10^{-4}\ M^{-1}\ s^{-1}$$

Based on all the kinetic calculations using UV–Visible and ^{1}H NMR reaction monitoring, we propose the following catalytic mechanism (Scheme 2). The catalyst (precursor) $([Co^{III}(tren)Cl_2]Cl)_2{\cdot}(Cl)(H_7O_3)$ (**$(1)_2{\cdot}(Cl)(H_7O_3)$**), reacts with LiOH to give the active catalytic species, $[Co^{III}(L)(OH)(H_2O)]^{2+}$, the formation of which is quite well documented in literature[41,44]. This active catalytic species then hydrolyses urea to yield ammonia and possibly isocyanic acid, which coordinates to the metal centre yielding $[Co^{III}(tren)(NH_3)(NCO)]Cl_2$ (**2**), the formation of which was confirmed by SC–XRD studies. However, the formation of $[Co^{III}(tren)(NH_3)(NCO)]Cl_2$ (**2**) is reversible, otherwise it would lead to catalyst poisoning rendering the catalyst inactive for the next catalytic cycle; our reactions worked even at 1:1000 catalyst to substrate ratio, indicating the catalytic nature of the reaction. The possibility of catalyst poisoning is also negated by the fact that the order of the reaction with respect to the catalyst was found to be close to unity. However, it must also be noted that no signal due to the isocyanato carbon could be observed in the reaction mixture even after 12 hr of reaction time. Interestingly, most synthetic Urease models coordinate urea via the carbonyl oxygen resulting in the formation of cyanato complexes and the liberation of ammonia. However, the coordination of urea to the metal centre via one of the nitrogen atoms has also been observed in a few cases, especially with soft metal centres. Some of these reports also account for an increased tendency of the coordinated urea to decompose into ammonia and carbon dioxide[14,29,45]. A similar elimination reaction pathway is proposed to operate in our reactions as well. The reaction is initiated by the coordination of urea to the Co(III) centre through nitrogen which is followed by a subsequent electrophilic attack by the coordinated hydroxide ligand onto the carbonyl carbon of urea (Scheme 2). This coordination of urea is substantiated by the isolation of $[Co^{III}(tren)(NH_3)(NCO)]Cl_2$ (**2**). Thus, we can conclude that $([Co^{III}(tren)Cl_2]Cl)_2{\cdot}(Cl)(H_7O_3)$ (**$(1)_2{\cdot}(Cl)(H_7O_3)$**) successfully hydrolyses the amide bond in urea to give ammonia and possibly a molecule of isocyanic acid. The liberation of ammonia and the subsequent increase in reaction pH was confirmed and monitored by UV–Visible spectroscopy. However, the exact fate of isocyanic acid and/or its decomposition into carbon dioxide could not be ascertained unambiguously. All the determined kinetic data has been compiled in Table 1.

Table 1. Kinetic data obtained for the catalytic hydrolysis of urea catalysed by $[Co(tren)Cl_2]Cl$ at pH 9 ± 0.05, in the presence of LiOH, at 45 °C.

Catalyst	k_{obs}	Ea*	TOF h^{-1} (TON)
$([Co^{III}(tren)Cl_2]Cl)_2{\cdot}(Cl)(H_7O_3)$, (**$(1)_2{\cdot}(Cl)(H_7O_3)$**)	3.89×10^{-4} M^{-1} s^{-1}	10.2 kJ mol^{-1}	1.2 (14.11)

* The activation energy corresponds to only the genration of ammonia and does not necessarily relate to the overall reaction.

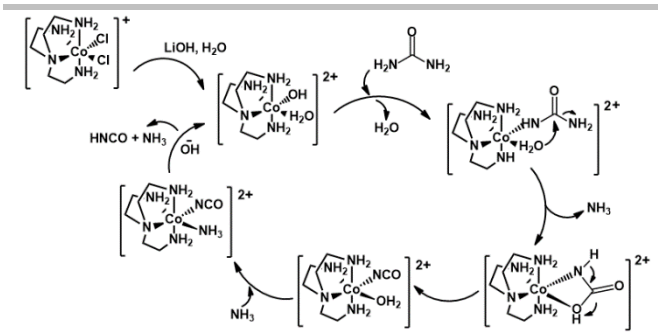

Scheme 2. Proposed mechanism for the hydrolysis of urea by [Co(tren)Cl_2]Cl at pH 9 ± 0.05, in the presence of LiOH, at 45 ºC (showing urea attack *via* nitrogen atom)

Structural characterization

***Bis-(dichloro(tris-2-amino(ethylamine))cobalt(III) chloride) hydroxonium chloride,* ([Co^{III}(tren)Cl_2]Cl)$_2$·(Cl)(H_7O_3), ((1)$_2$·(Cl)(H_7O_3))**

Complex II, [2($C_6H_{18}Cl_2CoN_4Cl_2$)·2H_2O H_3O^+ Cl^-], is a dimeric neutral Co(III) complex bearing two tris(2-aminoethyl)amine (*tren*) ligands coordinated to two Co(III) cations. Charge balance on the Co(III) occurs via four coordinated and two free Cl^- anions; one hydroxonium (H_3O^+) cation is found to be present in the structure and this cation is charge balanced with one chloride anion. There are also two water molecules present, both of which are adjacent to the H_3O^+, yielding a combined hydroxonium ionic aggregate of the form $H_7O_3^+$, which stabilizes the entire structure. The complex crystallizes in the centrosymmetric space group, $P2_1/n$ (see Figure 8). As mentioned above, this complex is an example of a molecular ionic aggregate as described by Bernal and Watkins[47] in the form $H_7O_3^+$. This is derived from the fact that the hydroxonium ion hydrogen bonds to the two water molecules resulting in three oxygen atoms and seven hydrogen atoms in the aggregate. As previously mentioned, the hydroxonium cation is charged balanced by a corresponding chloride anion. In each of the cations, there are four N atoms of the *tren* ligand that bind to one each of the Co(III) atoms in a quadridentate mode, resulting in a tripodal-type conformation with Co−N bond distances ranging from 1.935(2) – 1.966(2) Å. The coordination environment of the both of the Co(III) atoms is observed to have distorted octahedral geometry where the bond angles range from 86.28(9) – 95.17(7) °. (Refer to the Supplementary Information for detailed geometrical parameters). These distances and angles are similar to related complexes that have been published previously where a full geometry check carried out with the *Mogul* Geometry Check tool[46], within the CSD suite of programs, showed no unusual geometrical parameters.

There is evidence of hydrogen bonding present in this structure (see Figure 8 – indicated by the dashed lines). Details of the hydrogen bonding geometry appears in Table 2 below:

Table 2. Hydrogen-bond geometry of [Co^{III}(tren)Cl_2]Cl)$_2$·(Cl)(H_7O_3), **(1)$_2$·(Cl)(H_7O_3)** (Å, º)

D—H···*A*	*D*—H	H···*A*	*D*···*A*	*D*—H···*A*
N2—H2*A*···Cl4^{i}	0.87 (1)	2.69 (2)	3.417 (2)	142 (2)
N2—H2*B*···Cl1^{ii}	0.88 (1)	2.58 (2)	3.331 (2)	144 (2)
N3—H3*A*···Cl2^{i}	0.87 (1)	2.65 (2)	3.380 (2)	143 (2)
N3—H3*B*···Cl7^{i}	0.88 (1)	2.43 (2)	3.290 (2)	165 (3)
N4—H4*A*···Cl1^{ii}	0.86 (1)	2.66 (2)	3.483 (2)	161 (3)
N4—H4*B*···Cl7^{i}	0.86 (1)	2.53 (2)	3.281 (2)	146 (2)
N6—H6*C*···Cl6^{iii}	0.90 (3)	2.58 (3)	3.325 (3)	141 (2)
N6—H6*D*···Cl5^{iii}	0.73 (3)	2.68 (3)	3.359 (3)	155 (3)
N7—H7*A*···Cl7^{iv}	0.88 (1)	2.45 (2)	3.270 (2)	154 (2)
N7—H7*B*···Cl5^{iii}	0.87 (1)	2.41 (1)	3.279 (2)	176 (3)
N8—H8*A*···Cl2^{i}	0.88 (1)	2.54 (2)	3.409 (2)	170 (2)
N8—H8*B*···Cl7^{iv}	0.88 (1)	2.57 (2)	3.425 (2)	165 (2)
O1*S*—H1*SA*···Cl5^{v}	0.85 (1)	2.16 (2)	2.997 (2)	169 (3)
O1*S*—H1*SB*···O2S^{vi}	0.86 (1)	1.62 (2)	2.472 (3)	177 (3)
O1*S*—H1*SC*···O3S^{i}	0.86 (1)	1.61 (2)	2.460 (3)	173 (3)
O2*S*—H2*SA*···Cl5^{iv}	0.85 (1)	2.26 (2)	3.098 (2)	173 (3)
O2*S*—H2*SB*···Cl6^{i}	0.85 (1)	2.16 (2)	2.991 (2)	166 (3)
O3*S*—H3*SA*···Cl6^{i}	0.83 (1)	2.20 (2)	3.021 (2)	170 (3)
O3*S*—H3*SB*···Cl7	0.84 (1)	2.35 (2)	3.134 (2)	155 (3)

Symmetry codes: (i) −*x*+1, −*y*+1, −*z*+1; (ii) −*x*+3/2, *y*+1/2, −*z*+3/2; (iii) *x*, *y*−1, *z*; (iv) −*x*+1/2, *y*−1/2, −*z*+1/2; (v) −*x*+1/2, *y*−1/2, −*z*+3/2; (vi) −*x*+1, −*y*, −*z*+1.

The classification of this structure as a molecular ionic aggregate comes from the analysis of the hydrogen-bonding pattern that arises from a chain of hydrogen bonding evident between a centralized hydroxonium cation and two adjacent water molecules (see Figure 8). This structure fits in perfectly with the previous analysis[47] carried out, especially for $H_7O_3^+$ cases. The O···O distance between O1S and O2S = 2.472(3) Å and between O1S and O3S = 2.460(3) Å, which fits their description and analysis of these complexes and thus adds to their work on these aggregates.

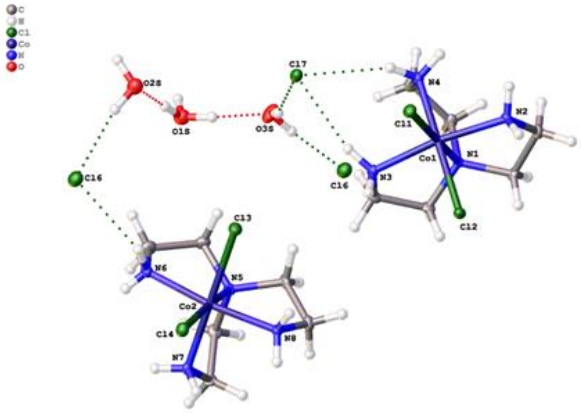

Figure 8. Molecular structure of ($[Co^{III}(tren)Cl_2]Cl)_2 \cdot (Cl)(H_7O_3)$, (**(1)$_2$·(Cl)($H_7O_3$)**) with displacement ellipsoids drawn at 50% probability, showing the atomic numbering scheme where the heteroatoms have been labelled only for clarity. Dashed red and green lines indicate hydrogen bonds.

Ammonio(tris-2-amino(ethylamine))isocyanatocobalt(III) dichloride **$[Co^{III}(tren)(NCO)(NH_3)]Cl_2$ (2)**

Complex III, $[C_7H_{21}CoN_6O \cdot 2(Cl)]$, is a neutral Co(III) complex bearing one tris(2-aminoethyl)amine (*tren*) ligand coordinated to the Co(III) cation. Charge balance on the Co(III) occurs via one coordinated isocyanato group (NCO^-) and two free Cl^- anions. The complex crystallizes in the centrosymmetric space group, *Pnma* (see Figure 9). A portion of this crystal structure exhibits disorder – atoms N4, C4 and C5 (together with their bonded H-atoms) are disordered over a mirror plane and the occupancies for these atoms have been refined to 0.5. For the cation, there are five N atoms of the *tren* ligand that bind to the Co(III) atom in a quadridentate mode, resulting in a tripodal-type conformation with Co−N bond distances ranging from 1.920(3) – 1.960(2) Å. There is a sixth N atom coordinated to the Co(III) atom in the form of an ammonio-group (NH_3). We postulate that the ammonio-coordination results from the fact that NH_3 is generated from the cleavage of the amide bond of urea and because Co has a high nitrogen affinity, coordination results from the free NH_3 generated. The coordination environment of the Co(III) atom is observed to have distorted octahedral geometry where the bond angles range from 86.54(8) – 93.49(8) °. (Refer to the Supplementary Information for detailed geometrical parameters). These distances and angles unfortunately could not be compared to other related structures in the CSD as this complex is the first Co(III) isocyanato compound reported of its kind. A full geometry analysis was performed with the *Mogul* Geometry Check tool[46], within the CSD suite of programs. This analysis yielded, in many instances, no comparable hits while unusual geometrical parameters were highlighted simply because the database had nothing to actually compare the geometry with.

There is evidence of hydrogen bonding present in this structure (see Figure 9 – indicated by the dashed lines). Details of the hydrogen bonding geometry appears in Table 3 below:

Table 3. Hydrogen-bond geometry of $[Co^{III}(tren)(NCO)(NH_3)]Cl_2$ (**2**) (Å, º)

D—H···*A*	*D*—H	H···*A*	*D*···*A*	*D*—H···*A*
N3—H3*A*···Cl1^{ii}	0.88 (1)	2.47 (2)	3.243 (3)	146 (3)
N3—H3*B*···Cl1^{i}	0.88 (1)	2.40 (2)	3.232 (3)	160 (3)
N6—H6*A*···Cl1^{ii}	0.88 (2)	2.50 (5)	3.326 (2)	157 (10)
N6—H6*B*···Cl1^{iii}	0.88 (2)	2.46 (4)	3.326 (2)	168 (14)
N6—H6*C*···O1^{iv}	0.87 (2)	2.10 (2)	2.952 (5)	167 (4)
N4—H4*A*···Cl1	0.88 (2)	2.34 (2)	3.2222 (16)	177 (6)
N4—H4*B*···Cl1^{i}	0.88 (2)	2.58 (4)	3.2222 (16)	131 (5)

Symmetry codes: (i) *x*, −*y*+1/2, *z*; (ii) −*x*+1/2, *y*−1/2, *z*+1/2; (iii) −*x*+1/2, −*y*+1, *z*+1/2; (iv) *x*, *y*, *z*−1.

The yield of this material was extremely low with only a few single crystals obtained and therefore this complex was only characterized by Single-crystal X-ray Diffraction. There was insufficient material for analyses by FTIR, NMR and UV-VIS.

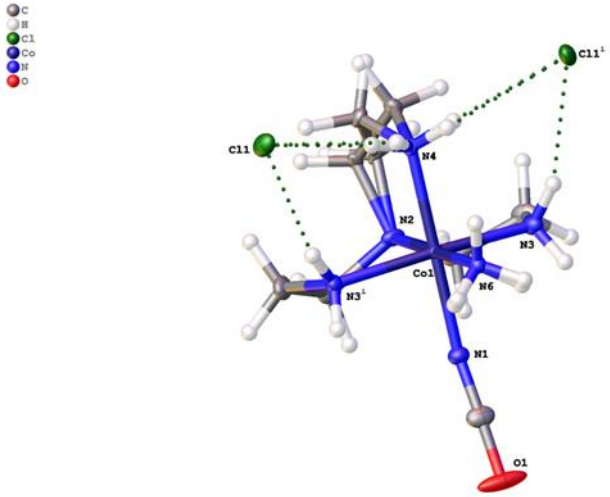

Figure 9. Molecular structure of $[Co^{III}(tren)(NCO)(NH_3)]Cl_2$ (**2**) with displacement ellipsoids drawn at 50% probability, showing the atomic numbering scheme where the heteroatoms have been labelled only for clarity, and showing the atoms that are disordered across the mirror plane. Dashed green lines indicate hydrogen bonds.

Conclusions

$[Co^{III}(tren)Cl_2)]Cl$ can be prepared in excellent yields following a two step synthetic protocol using $CoCl_2.6H_2O$ and tris(2-aminoethyl)amine (tren) under ambient conditions. The solvent used for crystallization plays a crucial role in stabilizing the resulting compound by involvement in intermolecular H bonding. The complex isolated by crystallizing in water, displays a rare hydroxonium $(H_7O_3)^+$ molecular ion aggregate mediated by extensive hydrogen bonding, which stabilizes the dimeric asymmetric unit by intermolecular H bonds.

The said compound successfully cleaves urea, following a dissociation mechanism forming isocyanic acid and ammonia. The isocyanic acid then coordinated to the metal centre and was

isolated as an isocyanato complex (**2**). The products are eventually released, generating the catalytic species available for the next catalytic cycle. Although, the results are similar to some of the reported Urease mimics in literature, to the best of our knowledge, the cobalt-isocyanato complex (**2**) is the first of its kind to be reported in literature. The reaction mechanism does not fit well into the Michaelis-Menten enzyme kinetics equation. Nevertheless, the reaction follows a first order kinetics with respect to both urea as well as the catalyst.

Experimental Section

Materials and instrumentation

All chemicals were used as received without further purification and were of the analytical grade. $CoCl_2.6H_2O$(Sigma Aldrich), tris(2–aminoethyl)amine (Sigma Aldrich), Urea (Saarchem) were used as obtained. FT-IR spectra were recorded in Attenuated total reflection mode on a Spectrum BX, Perkin Elmer FT–IR spectrometer. Electronic spectra of complexes were recorded in water on a Shimadzu 1800 UV–Vis spectrophotometer. ^{1}H NMR and ^{13}C NMR spectra were recorded in D_2O/CH_3OD on a Bruker Ultrashield 400 Nuclear Magnetic Resonance Spectrometer. NMR kinetics were performed on a Bruker Ascend 500 Nuclear Magnetic Resonance Spectrometer. High resolution mass spectra (HRMS) in positive ion electrospray ionization mass spectrometry mode were obtained on a Waters Synapt G2 mass spectrometer in CH_3CN. SCXRD data were obtained on a Bruker Apex – II Duo CCD diffractometer.

Syntheses

[Co(tren)(NO_2)$_2$]Cl (1a): $NaNO_2$ (7.2664 g, 0.105 mol) was added to a solution of $CoCl_2{\cdot}6H_2O$ (11.9819 g, 0.05 mol) in 10 mL deionised H_2O in a 100 mL side–arm flask. To this solution, a solution of HCl (4.4 mL, 32%) and 7.5 mL tris(2–aminoethyl)amine (tren) in 10 mL deionised H_2O was added and placed in an ice bath. Air oxidation was done for 2 hours and then a yellow–brown product was obtained and collected by suction filtration. The product was recrystallized in a minimum amount of warm water and recovered by suction filtration and dried. Yield: 9.7931 g, 67.3%. Selected IR bands (Figure S4) (νmax, cm–1): ν(N–H): 3281, 3156, 3091; ν(N–O) 1589; ν(CH_2) 1474; ν(NO_2) 1339, 1304; ν(C–N) 1146; ν(NH) 827; ν(CH_2) 745. UV-Vis (Figure S10) (H_2O): 438 nm (ε, 46.33 M^{-1} cm^{-1}), 322 nm (ε, 788 M^{-1} cm^{-1}). ^{1}H NMR (Figure S5) (D_2O, 400MHz): δ (ppm) 3.48 – 3.24 (m, 8H, –N–CH_2–CH_2–N–), 3.08 – 3.01 (m, 4H, –N–CH_2–CH_2–NH_2). ^{13}C NMR (Figure S6) (D_2O + CH_3OD, 400 MHz): δ (ppm) 62.46, 60.22, 44.43.

([Co^{III}(tren)Cl_2]Cl)$_2$·(Cl)(H_7O_3) ((1)$_2$·(Cl)(H_7O_3)): [Co(tren)(NO_2)$_2$]Cl (7.0008 g, 0.021 mol) was added into a 100 mL beaker and then 32% HCl (50 mL) was added to it. The solvent was then evaporated on a hot water bath to dryness and then the precipitate was dissolved in a minimum amount of warm deionised H_2O. The precipitate was isolated by vacuum filtration and washed with cold deionised H_2O and MeOH. Yield: 5.9011 g, 90%. Selected IR bands (Figure S7) (νmax, cm^{-1}): ν(N–H): 3234, 3135, 3081; ν(CH_2) 1591, 1480; ν(C–N) 1160, 1032; ν(NH) 896; ν(CH_2) 743. UV-Vis (Figure S10) (H_2O): 533 nm (ε, 561 M^{-1} cm^{-1}), 370 nm (ε, 385 M^{-1} cm^{-1}). ^{1}H NMR (Figure S8) (D_2O, 400MHz): δ (ppm). 3.60 – 3.56 (m, 2H, –N–CH_2–CH_2–N–), 3.39 – 3.32 (m, 4H, –N–CH_2–CH_2–N–), 3.25 – 3.22 (t, 2H, –N–CH_2–CH_2–N–), 2.86 – 2.82 (m, 2H, –N–CH_2–CH_2–N–), 2.74 – 2.70 (t, 2H, –N–CH_2–CH_2–N–). ^{13}C NMR (Figure S9) (D_2O + CH_3OD, 400 MHz): δ (ppm) 61.04, 60.00, 44.63, 43.47.

[Co^{III}(tren)(NH_3)(NCO)]Cl_2 (2): Urea (1.0020 g, 17 mmol) was dissolved in 30 mL deionised H2O and then [Co(tren)Cl2]Cl (0.535 g, 0.75 mmol) was added to the stirring solution. The pH of the solution was adjusted to 9.0 with freshly prepared 10% LiOH and then stirred at 40 ºC for 2 hours. The reaction was allowed to cool to room temperature and then left to stand and evaporate at room temperature for a couple of days after which orange rod–like crystals suitable for SC–XRD precipitated out. The concentrations of LiOH used for pH regulations were adjusted according to the concentration of the catalyst used for analysis to obtain a pH range of 9 – 9.2.

Catalytic hydrolysis of Urea as monitored by ^{1}H NMR

A solution of ([Co^{III}(tren)Cl_2]Cl)$_2$·(Cl)(H_7O_3), (**(1)$_2$·(Cl)(H_7O_3)**) (0.124 g, 0.17 mmol) in 10 mL D_2O was incubated at pH 9 ± 0.05 for 2 h in the presence of LiOH. Urea (0.240 g, 4.0 mmol) was added to this solution, and 0.5 mL of the solution was sealed in an NMR tube and the solution was maintained at 45 ˚C for about 12 h. The progress of reaction was monitored by recording ^{1}H NMR spectra of the reaction mixture every 15 minutes.

Catalytic hydrolysis of Urea as monitored by UV–Vis

The Ureases activity of ([Co^{III}(tren)Cl_2]Cl)$_2$·(Cl)(H_7O_3) (**(1)$_2$·(Cl)(H_7O_3)**) was also analysed by monitoring the release of NH_3 by use of suitable dye indicators – phenolphthalein. Therefore, the reaction was followed employing UV–Visible spectroscopy by monitoring the absorbance increment at 552 nm due the alkaline quinone form of phenolphthalein. The reaction was initiated by adding an aqueous solution of Urea (2 mL, 1 × 10^{-2} M) to an aqueous solution of ((1)$_2$·(Cl)(H_7O_3)) (2 mL, 4.5 × 10^{-3} M) pH incubated at 9 ± 0.05 with 1 % LiOH solution in water. Phenolphthalein (1 mL, 1%) was added to this reaction mixture, and it was incubated at 45 ˚C. The UV–Visible spectrum of the resulting reaction mixture was then recorded every 2 minutes as a function of time in repeat scan mode for 2 h. Steady state kinetics was performed similarly over a period of 3 minutes at different temperatures ranging from 20 ˚C to 50 ˚C, and the initial rates were calculated from the slope of absorbance vs time plots. The initial rates were then fitted to Arrhenius plot to calculate activation energy E_a for the reaction from nonlinear curve fit using Origin 8.0 software. The stability of the indicator, phenolphthalein at the reaction pH was monitored by UV/Vis spectroscopy (see Figure S 11).

Single Crystal Data - Experimental

***Dichloro(tris-2-amino(ethylamine))cobalt(III) chloride hydrate,* [Co^{III}(tren)Cl_2]Cl·H_2O, (1·H_2O)**

Single purple block-shaped crystals of Complex I were obtained by recrystallisation from concentrated hydrochloric acid (32% solution). A suitable crystal (0.27×0.18×0.13) mm^3 was selected and mounted on the tip of a MiTeGen MicroMount© and then placed on a Bruker APEX-II CCD diffractometer. The crystal was kept at T = 100(2) K during data collection. Using *Olex2*[48], the structure was solved with the *ShelXT 2014/5*[49,50] structure solution program, using the Intrinsic Phasing solution method. The model was refined with *ShelXL-2017/1*[49,50] using Least Squares minimisation.
A detailed structural description is included in the SI.

***Bis-(dichloro(tris-2-amino(ethylamine))cobalt(III) chloride hydroxonium chloride,* ([Co^{III}(tren)Cl_2]Cl)$_2$·(Cl)(H_7O_3), ((1)$_2$·(Cl)(H_7O_3))**

Single clear dark violet plank-shaped crystals of Complex II were obtained by recrystallisation from water. A suitable crystal (0.39×0.29×0.20) mm^3 was selected and mounted on the tip of a MiTeGen MicroMount©.and then placed on a Bruker APEX-II CCD diffractometer. The crystal was kept at T = 100.1 K during data collection. Using *Olex2*[48] the structure was solved

with the *ShelXS–97*[49,50] structure solution program, using the Direct methods solution method. The model was refined with *ShelXL-2017/1*[49,50] using Least Squares minimisation.

***Ammonio(tris-2-amino(ethylamine))isocyanatocobalt(II) chloride* [Co^{III}(tren)(NCO)(NH_3)]Cl_2 (2)**

Single clear dark brown block-shaped crystals of Complex III were obtained by recrystallisation from the mother liquor of the catalytic reaction mixture. A suitable crystal (0.15×0.14×0.14) mm^3 was selected and mounted on the tip of a MiTeGen MicroMount©.and then placed on a Bruker APEX-II CCD diffractometer. The crystal was kept at T = 100(2) K during data collection. Using *Olex2*[48], the structure was solved with the *ShelXS–97*[49,50] structure solution program, using the Direct methods solution method. The model was refined with *ShelXL-2017/1*[49,50] using Least Squares minimisation.

Single Crystal Data and Structure Quality Indicators

***Bis-(dichloro(tris-2-amino(ethylamine))cobalt(III) chloride) hydroxonium chloride,* ([Co^{III}(tren)Cl_2]Cl)$_2$·(Cl)(H_7O_3), ((1)$_2$·(Cl)(H_7O_3))**

$C_{12}H_{43}Cl_7Co_2N_8O_3$, M_r = 713.55, monoclinic, $P2_1/n$ (No. 14), a = 19.732(3) Å, b = 8.0255(12) Å, c = 20.161(3) Å, β = 118.466(3)°, $\alpha = \gamma$ = 90°, V = 2806.7(7) Å^3, T = 100.1 K, Z = 4, Z' = 1, μ(MoK$_a$) = 1.879, 39625 reflections measured, 7021 unique (R_{int} = 0.0830) which were used in all calculations. The final wR_2 was 0.0770 (all data) and R_1 was 0.0356 (I > 2(I)). Data were measured using ϕ and ω scans of 0.50 ° per frame for 10 s using MoKα radiation (graphite monochromated, 50 kV, 30 mA). The total number of runs and images was based on the strategy calculation from the program APEX2[51]. The maximum resolution achieved was Θ = 28.387°. Cell parameters were retrieved using *SAINT*[52] software and refined using *SAINT*[52] on 3885 reflections, 10 % of the observed reflections. Data reduction was performed using the *SAINT*[52] software which corrects for Lorentz polarisation. The final completeness is 100.00 % out to 28.387° in Θ. A multi-scan absorption correction was performed using *SADABS-2012/1*[54] was used for absorption correction. wR_2(int) was 0.0728 before and 0.0648 after correction. The ratio of minimum to maximum transmission is 0.8776. The λ/2 correction factor is 0.0015. The absorption coefficient μ of this material is 1.879 mm^{-1} at this wavelength (λ = 0.71073Å) and the minimum and maximum transmissions are 0.6544 and 0.7457. Structure refinement was carried out such that all non-hydrogen atoms were refined anisotropically Most hydrogen atom positions were calculated geometrically and refined using the riding model, but some hydrogen atoms were refined freely. The H atoms that were allowed to refine freely were, in most cases, restrained by DFIX parameters as their refinement had a slight tendency to become unstable, resulting in unequal N−H bond lengths.

***Ammonio(tris-2-amino(ethylamine))isocyanatocobalt(III) dichloride* [Co^{III}(tren)(NCO)(NH_3)]Cl_2 (2)**

$C_7H_{21}Cl_2CoN_6O$, M_r = 335.13, orthorhombic, *Pnma* (No. 62), a = 16.162(3) Å, b = 11.562(2) Å, c = 7.1615(12) Å, $\alpha = \beta = \gamma$ = 90°, V = 1338.2(4) Å^3, T = 100(2) K, Z = 4, Z' = 0.5, μ(MoK$_a$) = 1.677, 12702 reflections measured, 1763 unique (R_{int} = 0.0810) which were used in all calculations. The final wR_2 was 0.1053 (all data) and R_1 was 0.0414 (I > 2(I)). Data were measured using ϕ and ω scans of 0.50 ° per frame for 10 s using MoKα radiation (graphite monochromated, 50 kV, 30 mA). The total number of runs and images was based on the strategy calculation from the program APEX2[51]. The maximum resolution achieved was Θ = 28.391°. Cell parameters were retrieved using *SAINT*[52] software and refined using *SAINT*[52] on 1483 reflections, 12 % of the observed reflections. Data reduction was performed using the *SAINT*[52] software which corrects for Lorentz polarisation. The final completeness is 100.00 % out to 28.391° in Θ. A multi-scan absorption correction was performed using *SADABS-2012/1*[54] was used for absorption correction. wR_2(int) was 0.0695 before and 0.0645 after correction. The ratio of minimum to maximum transmission is 0.8852. The λ/2 correction factor is 0.0015. The absorption coefficient μ of this material is 1.677 mm^{-1} at this wavelength (λ = 0.71073Å) and the minimum and maximum transmissions are 0.6602 and 0.7458. Structure refinement was carried out such that all non-hydrogen atoms were refined anisotropically Most hydrogen atom positions were calculated geometrically and refined using the riding model, but some hydrogen atoms were refined freely. The value of Z' is 0.5. This means that only half of the formula unit is present in the asymmetric unit, with the other half consisting of symmetry equivalent atoms.

Some details of the crystal structure determination are also given in Table 5. CCDC 1848991 ([Co^{III}(tren)Cl_2]Cl·H_2O, (**1·H_2O**)), 1848992 (([Co^{III}(tren)Cl_2]Cl)$_2$·(Cl)(H_7O_3) (**(1)$_2$·(Cl)(H_7O_3)**)) and 1848993 ([Co^{III}(tren)(NH_3)(NCO)]Cl_2 (**2**)) contain the supplementary crystallographic data for the structures reported in this paper. These data can be obtained free of charge via http://www.ccdc.cam.ac.uk/conts/retrieving.html, or from the Cambridge Crystallographic Data Centre, 12 Union Road, Cambridge CB2 1EZ, UK; fax: (+44) 1223 336 033; or e–mail: deposit@ccdc.cam.ac.uk. Supplementary data associated with this article can be found, in the online version, at doi: $$$$$.

Table 5. Crystal data and structure refinement for ([Co^{III}(tren)Cl_2]Cl)$_2$·(Cl)(H_7O_3) (**(1)$_2$·(Cl)(H_7O_3)**), [Co^{III}(tren)(NH_3)(NCO)]Cl_2 (**2**)

	(1)$_2$·(Cl)(H_7O_3)	**(2)**
Formula	2($C_6H_{18}Cl_2CoN_4$)·3(Cl)·H_3O·2(H_2O)	$C_7H_{21}CoN_6O$·2(Cl)
T	100 K	100 K
Wavelength, Å	0.71073 Å	0.71073 Å
Formula weight	713.55	335.13
Crystal System	Monoclinic	Orthorhombic,
Space Group	$P2_1/n$	*Pnma*
a	19.732 (3) Å	16.162 (3) Å
b	8.0255 (12) Å	11.562 (2) Å
c	20.161 (3) Å	7.1615 (12) Å
β	118.466 (3)°	
V	2806.7 (7) Å^3	1338.2 (4) Å^3
Z	4	4
F(000)	1472	696

D_x	1.689 Mg m^{-3}	1.663 Mg m^{-3}
μ	1.88 mm^{-1}	1.68 mm^{-1}
θ	2.3–28.3°	2.5–26.5°
R_{int}	0.083	0.081
Crystal Size	0.39 × 0.30 × 0.20 mm	0.15 × 0.14 × 0.14 mm
Goodness–of–fit on F^2	1.01	1.01
$R[F^2 > 2\sigma(F^2)]$	0.036	0.041
wR_2 (all data) [b]	0.077	0.105
Largest differences peak and hole (eÅ^{-3})	0.59 and –0.57	2.74 and –0.53

Acknowledgements

The authors acknowledge the University of Johannesburg and the NRF Thuthuka Programme (Grant no: 99164) for funding for this study. Mr. D. Harris and Dr R. Meyer from Shimadzu South Africa are also gratefully acknowledged for the equipment (UV-Visible spectrometer) we used to conduct this project.

Keywords: cobalt complexes • kinetics • stucture elucidation • urea • urease activity

References

[1] L. S. B. Upadhyay, *Indian J. Biotechnol.* **2012**, *11*, 381–388.
[2] W. Z. Lee, H. S. Tseng, T. L. Wang, H. L. Tsai, T. S. Kuo, *Organometallics* **2010**, *29*, 2874–2881.
[3] E. L. Carter, N. Flugga, J. L. Boer, S. B. Mulrooney, R. P. Hausinger, *Metallomics* **2009**, *1*, 207–221.
[4] H. L. Mobley, M. D. Island, R. P. Hausinger, *Microbiol. Rev.* **1995**, *59*, 451–480.
[5] Z.-L. You, L.-L. Ni, D.-H. Shi, S. Bai, *Eur. J. Med. Chem.* **2010**, *45*, 3196–3199.
[6] H. Deng, G. Hong, F. Lin, A. Liu, X. Xia, W. Chen, *Anal. Chim. Acta* **2016**, *915*, 74–80.
[7] G. Estiu, K. M. Merz, *J. Am. Chem. Soc.* **2004**, *126*, 11832–11842.
[8] Y. Cui, X. Dong, Y. Li, Z. Li, W. Chen, *Eur. J. Med. Chem.* **2012**, *58*, 323–331.
[9] P. A. Karplus, M. A. Pearson, R. P. Hausinger, *Acc. Chem. Res.* **1997**, *30*, 330–337.
[10] M. N. Belzile, A. A. Neverov, R. S. Brown, *Inorg. Chem.* **2014**, *53*, 7916–7925.
[11] D. A. Daramola, D. Singh, G. G. Botte, *J. Phys. Chem. A* **2010**, *114*, 11513–11521.
[12] G. Estiu, K. M. Merz, *J. Phys. Chem. B* **2007**, *111*, 10263–10274.
[13] B. Krajewska, *J. Mol. Catal. B Enzym.* **2009**, *59*, 9–21.
[14] M. Belzile, A. A. Neverov, R. S. Brown, *Inorg. Chem.* **2014**, *53*, 7916−7925.
[15] B. P. Callahan, Y. Yuan, R. Wolfenden, *J. Am. Chem. Soc.* **2005**, *127*, 10828–10829.
[16] J. F. Marlier, L. I. Robins, K. A. Tucker, J. Rawlings, M. A. Anderson, W. W. Cleland, *Biochemistry* **2010**, *49*, 8213–8219.
[17] I. S. Park, R. P. Hausinger, *Biochemistry* **1996**, *35*, 5345–5352.
[18] F. Musiani, E. Arnofi, R. Casadio, S. Ciurli, *J. Biol. Inorg. Chem.* **2001**, *6*, 300–314.
[19] B. P. Roberts, B. R. Miller, A. E. Roitberg, K. M. Merz, *J. Am. Chem. Soc.* **2012**, *134*, 9934–9937.
[20] D. Volkmer, B. Hommerich, K. Griesar, W. Haase, B. Krebs, P. Chemie, T. H. Darmstadt, D.- Darmstadt, R. V December, H. O. C. H. O. Et, **1996**, *1669*, 3792–3803.
[21] A. Balasubramanian, K. Ponnuraj, *J. Mol. Biol.* **2010**, *400*, 274–283.
[22] B. Zambelli, F. Musiani, S. Benini, S. Ciurli, *Acc. Chem. Res.* **2011**, *44*, 520–530.
[23] F. Meyer, E. Kaifer, P. Kircher, K. Heinze, H. Pritzkow, *Chem. - A Eur. J.* **1999**, *5*, 1617–1630.
[24] W.-Z. Lee, H.-S. Tseng, M.-Y. Ku, T.-S. Kuo, *Dalt. Trans.* **2008**, *2*, 2538–2541.
[25] A. M. Barrios, S. J. Lippard, *J. Am. Chem. Soc.* **2000**, *122*, 9172–9177.
[26] T. Koga, H. Furutachi, T. Nakamura, N. Fukita, M. Ohba, K. Takahashi, H. Ōkawa, *Inorg. Chem.* **1998**, *37*, 989–996.
[27] Z. Khan, M. Z. A. Rafiquee, Kabir-ud-din, M. Arif Niaz, A. Aziz Khan, *Indian J. Chem. - Sect. A Inorganic, Phys. Theor. Anal. Chem.* **1996**, *35*, 1116–1119.
[28] A. M. Barrios, S. J. Lippard, *Inorg. Chem.* **2001**, *40*, 1250–1255.
[29] L. Roecker, J. Akande, L. N. Elam, I. Gauga, B. W. Helton, M. C. Prewitt, A. M. Sargeson, J. H. Swango, A. C. Willis, T. Xin, J. Xu, *Inorg. Chem.* **1999**, *38*, 1269–1275.
[30] C. te Grotenhuis, N. van den Heuvel, J. I. van der Vlugt, B. de Bruin, *Angew. Chemie - Int. Ed.* **2018**, *57*, 140–145.
[31] C. F. Harris, C. S. Kuehner, J. Bacsa, J. D. Soper, *Angew. Chemie - Int. Ed.* **2018**, *57*, 1311–1315.
[32] K. Kawai, Y. Bunno, T. Yoshino, S. Matsunaga, *Chem. - A Eur. J.* **2018**, *24*, 10231 – 10237.
[33] S. K. Ghosh, A. Ehnbom, K. G. Lewis, J. A. Gladysz, *Coord. Chem. Rev.* **2017**, *350*, 30–48.
[34] M. K. Saha, I. Bernal, *Chem. Commun.* **2003**, 612–613.
[35] M. K. Saha, U. Mukhopadhyay, I. Bernal, *Dalt. Trans.* **2004**, 1466–1473.
[36] U. Mukhopadhyay, R. Galian, I. Bernal, *Inorganica Chim. Acta* **2009**, *362*, 4237–4240.
[37] D. A. Buckingham, P. J. Cresswell, A. M. Sargeson, *Inorg. Chem.* **1975**, *14*, 1485–1490.
[38] I. A. Guzei, C. Arderne, *Acta Crystallogr. Sect. C Struct. Chem.* **2015**, *71*, 695–700.
[39] D. A. Buckingham, J. P. Collman, D. A. R. Happer, L. G. Marzilli, *J. Am. Chem. Soc.* **1967**, *89*, 1082–1087.
[40] D. A. Buckingham, J. P. Collman, *Inorg. Chem.* **1967**, *6*, 1803–1807.
[41] A. A. Phulambrikar, C. Chatterjee, *Order A J. Theory Ordered Sets Its Appl.* **2002**, *1519*, 1515–1519.
[42] B. Krajewska, R. Van Eldik, M. Brindell, *J. Biol. Inorg. Chem.* **2012**, *17*, 1123–1134.
[43] C.-F. Wang, Z.-J. Chen, K.-D. Zhao, X.-F. Chen, C.-Y. Zhang, G.-H. Sheng, H.-L. Zhu, *J. Coord. Chem.* **2016**, *69*, 2656–2665.
[44] R. W. Hay, N. Govan, *Transit. Met. Chem.* **1998**, *725*, 721–725.
[45] N. V. Kaminskaia, N. M. Kostic, *Inorg. Chem.* **1997**, *36*, 5917–5926.
[46] I. J. Bruno, J. C. Cole, M. Kessler, J. Luo, W. D. S. Momerwell, L. H. Purkis, B. R. Smith, R. Taylor, R. I. Cooper, S. E. Harris, A. G. Orpen, *J. Chem. Inf. Comput. Sci.* **2004**, *44*, 2133–2144.
[47] I. Bernal, S. F. Watkins, *Acta Crystallogr. Sect. C Struct. Chem.* **2014**, *70*, 566–574.
[48] O. V. Dolomanov, L. J. Bourhis, R. J. Gildea, J. A. K. Howard, H. Puschmann, *J. Appl. Crystallogr.* **2009**, *42*, 339–341.
[49] G. M. Sheldrick, *Acta Crystallogr. Sect. C Struct. Chem.* **2015**, *71*, 3–8.
[50] G. M. Sheldrick, *Acta Crystallogr. Sect. A Found. Crystallogr.* **2015**, *71*, 3–8.
[51] Bruker, **2014**., *APEX2, SAINT, SADABS,* Bruker AXS, Inc., Madison, Wisconsin, USA
[52] Bruker, **2013**., *APEX2, SAINT, SADABS,* Bruker AXS, Inc., Madison, Wisconsin, USA
[53] Bruker, **2016**., *APEX2, SAINT, SADABS,* Bruker AXS, Inc., Madison, Wisconsin, USA
[54] Bruker, **2012**., *APEX2, SAINT, SADABS,* Bruker AXS, Inc., Madison, Wisconsin, USA

WILEY-VCH

Entry for the Table of Contents

Layout 1:

FULL PAPER

We have explored the catalytic activity of $[Co^{III}(tren)Cl_2]Cl$ towards the cleavage of he amide bond in urea, with respect to Urease mimetic activity. The reaction kinetics were followed spectroscopically; and the formation of products was confirmed by SC XRD technique.

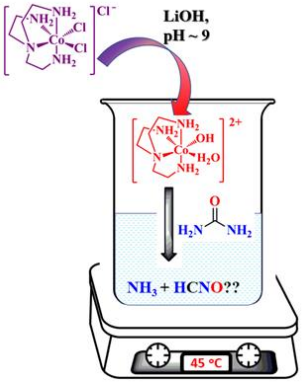

Enzyme Mimetics

Bhawna Uprety, Charmaine Arderne, Ivan Bernal, Charmaine Arderne**

Page No. – Page No.

Catalytic cleavage of the amide bond in urea using a Co(III) amino-based complex